Optical Gaps of Organic Solar Cells as a Reference for Comparing Voltage Losses

Yuming Wang, Deping Qian, Yong Cui, Huotian Zhang, Jianhui Hou, Koen Vandewal, Thomas Kirchartz and Feng Gao

Wang, Y., Qian, D., Cui, Y., Zhang, H., Hou, J., Vandewal, K., Kirchartz, T., Gao, F., (2018), Optical Gaps of Organic Solar Cells as a Reference for Comparing Voltage Losses, *ADVANCED ENERGY MATERIALS*, 8(28), 1801352. https://doi.org/10.1002/aenm.201801352

Original publication available at:
https://doi.org/10.1002/aenm.201801352

Optical Gaps of Organic Solar Cells as a Reference for Comparing Voltage Losses

Yuming Wang, Deping Qian, Yong Cui, Huotian Zhang, Jianhui Hou, Koen Vandewal, Thomas Kirchartz, Feng Gao**

Y. Wang, Dr. D. Qian, H. Zhang, Dr. F. Gao
Department of Physics, Chemistry and Biology (IFM), Linköping University,
SE-58183, Linköping, Sweden
E-mail: feng.gao@liu.se
Y. Cui, Prof. J. Hou
State Key Laboratory of Polymer Physics and Chemistry
Beijing National Laboratory for Molecular Sciences
CAS Research/Education Center for Excellence in Molecular Sciences
Institute of Chemistry
Chinese Academy of Sciences
100190, Beijing, China
Prof. K. Vandewal
Instituut voor Materiaalonderzoek (IMO-IMOMEC)
Hasselt University
Wetenschapspark 1
BE-3590, Diepenbeek, Belgium
Prof. T. Kirchartz
IEK5-Photovoltaik, Forschungszentrum Jülich
52425 Jülich, Germany
Prof. T. Kirchartz
Faculty of Engineering and CENIDE
University of Duisburg-Essen
Carl-Benz-Str. 199
47057 Duisburg, Germany
Email: t.kirchartz@fz-juelich.de

Key words: Organic solar cells, optical gap, voltage losses, Shockley-Queisser limit

Abstract

The voltage loss, determined by the difference between the optical gap (E_g) and the open-circuit voltage (V_{OC}), is one of the most important parameters determining the performance of organic solar cells (OSCs). However, the variety of different methods used to determine E_g makes it hard to fairly compare voltages losses among different material systems. In this paper, we discuss and compare various E_g determination methods and show how they affect the detailed calculation of the voltage losses, as well as predictions of the maximum achievable power conversion efficiency. The aim of this paper is to make it possible for the OSC community to compare the voltage losses in a consistent and reasonable way. We find that the voltage losses for strongly absorbed photons in state-of-the-art OSCs are not much less than 0.6 V, which are still to be decreased to further enhance the efficiency.

1. Introduction

The performance of organic solar cells (OSCs) has been steadily increasing over the past decades.[1-8] Efficient exciton dissociation and free charge carrier generation in OSCs is realized by utilizing heterojunctions formed by blending electron donor and electron acceptor materials.[9-11] Great efforts have been dedicated to materials engineering and device optimization.[12-22] As a consequence, photon absorption and conversion into electrical current have been improved remarkably, leading to the power conversion efficiencies (PCEs) approaching ~14% in single junction OSCs, with high external quantum efficiencies (*EQE* ~70-80%) and fill factors (reaching ~70-75%).[23-27] In particular, a whole range of non-fullerene acceptor molecules, such as 3,9-bis(2-methylene-(3-(1,1-dicyanomethylene)-indanone))-5,5,11,11-tetrakis(4-hexylphenyl)-dithieno[2,3-d:2',3'-d']-s-indaceno[1,2-b:5,6-b']dithiophene (ITIC) derivatives, have been developed in recent years, leading to substantially improved open-circuit voltages and efficiencies.[24, 28-34] In order to identify and compare progress in open-circuit voltage (V_{OC}) improvement, a direct comparison of the V_{OC} values is insufficient. Indeed, V_{OC} varies strongly with the energy of the charge-transfer state which is limited by the absorption onset of the donor and acceptor molecules.[35-42] Thus, the open-circuit voltage has to be considered with respect to a meaningful reference value, agreed upon by the community.

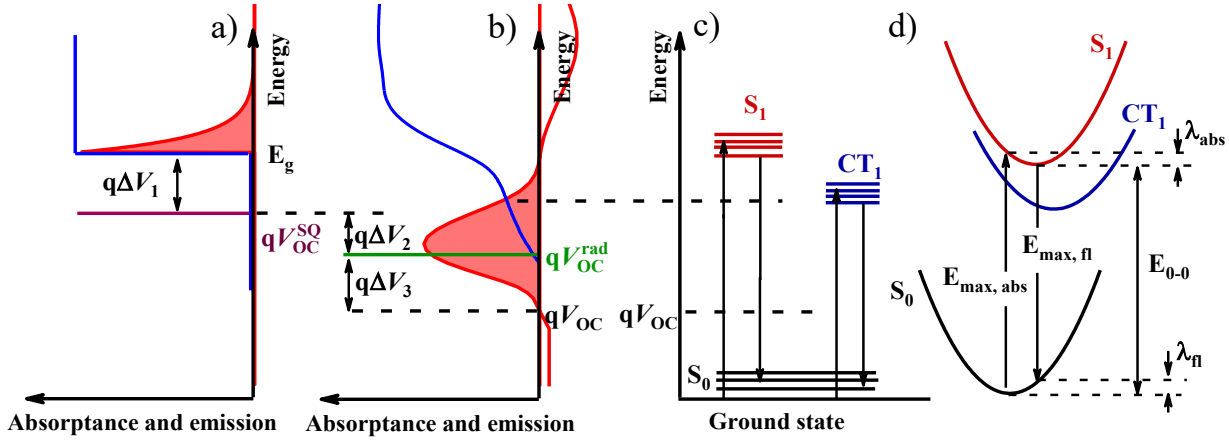

Figure 1. The absorptance (blue curves) and emission (red curves with pink shadow) of a) SQ type devices and b) real-word OSC devices. In contrast to the absorptance of SQ type devices, the absorptance of real-word OSCs is not a step-function. Instead, the absorptance is smeared out with weakly absorbing subgap features being due to absorption of the charge-transfer state. These weakly absorbing features often dominate emission (red). Here, we note that, in some novel material systems, the absorptance and emission of charge transfer states disappear, leading to significantly reduced voltage losses. c) Jablonski diagram of the active layer in OSCs. d) Diagram showing the energy of S_1, S_0 and CT_1 as a function of the configuration coordinate.

Shockley-Queisser (SQ) theory and its variations for realistic absorptance spectra have proven useful to obtain insights in the physical nature of voltage losses.[43-44] In the SQ limit, the only free parameters are the band gap and the temperature of the solar cell. The absorptance spectrum is simplified as a step-function as shown in **Figure 1**a with the band gap E_g as the threshold energy for the step. The emission spectrum equals the black body spectrum multiplied by this step function.

The maximum V_{OC} in the SQ limit is reduced by ΔV_1 with respect to E_g/q due to unavoidable radiative recombination losses. A non-ideal absorption spectrum, for example due to a non-abrupt absorption onset and the presence of sub-gap charge transfer states (**Figure 1**c, d), reduces voltage losses further by ΔV_2 (**Figure 1**b). In addition to these radiative losses, which are purely determined by the shape and spectral position of the absorption onset, non-radiative recombination reduces the open-circuit voltage further (ΔV_3).[45-48]

While a step-function always has a well-defined threshold energy, it is not trivial to assign a single value to characterize the onset of a measured absorptance. Indeed, the onset value varies depending on the definition and the method of obtaining it. In addition to relating the measured V_{OC} to its thermodynamic limit, it is common in the literature to relate V_{OC} directly to the optical gap. The voltage loss (ΔV_{OC}) is then determined by the difference between the E_g/q and the V_{OC}, (using various definitions of the gap as depicted in **Figure 2**). To date, a large number of papers related to "low" voltage losses have been published, in which voltage losses in the range of ~0.47

to 0.6 V were reported.[33, 44, 49-55] It should be noted that in these papers, the optical gaps of the devices were extracted in different ways, making direct comparisons tedious or impossible.[56]

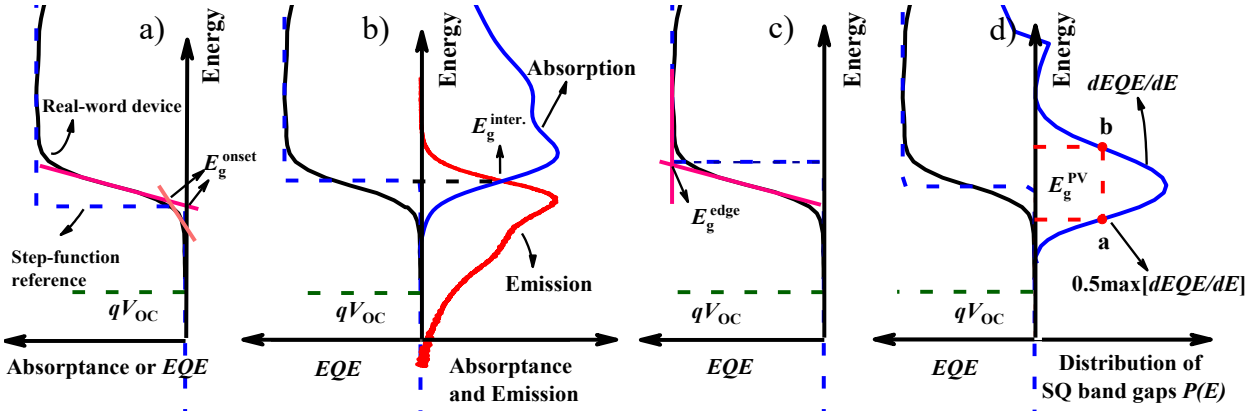

Figure 2. Different E_g determination methods. The step-functions (blue dash curves) are used as references for the absorptance or *EQE* (solid black curves) of real-word OSCs. a) E_g is determined from the absorptance or *EQE* onset, denoted as E_g^{onset}. b) E_g is determined at the intersection between absorptance (solid blue curve) and emission (solid red curve), denoted as $E_g^{inter.}$. c) E_g is determined by the crossing point of extrapolated line of the *EQE* edge and horizontal tangent of the local peak, denoted as E_g^{edge}. d) E_g is determined from the derivatives of the *EQE* curve, and a mean peak energy is calculated by the Equation 7, denoted as E_g^{PV}.

There are two strict definitions of "band gap" in the context of photovoltaics. The (i) purely mathematical definition of band gap as a threshold energy of a step-function in the Shockley-Queisser limit and (ii) the gap in the density of states of a perfectly periodic crystal. In a perfectly periodic crystal, the minimum energy to remove one valence electron from a bond and create a free electron is a constant. Any electronic states that still exist in the gap originate from interruptions of this perfect periodicity. Thus, any disordered amorphous or nano-crystalline semiconductor will still have an energetic region with an extremely low density of electronic states but there will be no perfect gap and therefore no strict definition of "band gap" would apply.[57] Any research community working on a photovoltaic technology based on disordered semiconductor absorbers would therefore have to develop practical definitions of "band gap" that serve the same purposes

as the strict definition in a monocrystalline semiconductor. Typically, these definitions are either motivated via the optical absorption (optical gap)[58-59] or the recombination and transport of charge carriers (i.e., the mobility gap).[57, 60-61] Some of these definitions may be useful for a certain technology despite being completely arbitrary. One example for a particularly arbitrary definition is the frequently used E_{04} gap in amorphous silicon, which is defined as the energy where the absorption coefficient exceeds 10^4 cm^{-1}.[59] Given the disordered nature of organic semiconductor blends used for organic photovoltaics, quite similar questions of how to define practical equivalents of the "band gap" arise. This is true in particular in the context of the above mentioned methods of analyzing open-circuit voltage losses. No matter what exact approach is used to quantify and compare voltage losses between different devices or material systems, there must be a clear consensus about how to define and determine band gaps that serve as suitable references. Nowadays, various definitions have been proposed to identify the optical gaps, while no consensus has been reached yet for a standard definition. These definitions differ in how easy they may be applied to experimental data, how reproducible the analysis is and how to interpret the resulting voltage losses. Thus, it is important to consider which definition is ideal for a certain purpose and how a different choice of optical gap definition affects the interpretation of data.

In this study, we discuss how previously reported definitions for E_g affect each part of the voltage loss quantification, as well as their strengths and weaknesses. We plot the peak *EQE* values (EQE_{max}) versus ΔV_{OC} for over thirty fullerene- and non-fullerene-containing material systems using the definitions that have been proposed in the literature. Regardless of the definition of E_g, we find that EQE_{max} is independent of ΔV_{OC} for both fullerene and non-fullerene acceptors, in contrast to the previous assumption that increasing ΔV_{OC} is beneficial to enhance the EQE_{max}.[62] However, the absolute voltage losses as well as predictions for efficiency upper limits are strongly

affected by the method of E_g determination. To date, no OSCs with a voltage loss for strongly absorbed photons significantly lower than 0.6 V has been reported. This leads to a prediction of a realistic efficiency upper limit of ~ 18 % for single-junction cells.

2. Different E_g values affecting the voltage loss quantification

Different E_g determination methods essentially assign differing references for comparing the V_{OC}. As shown in **Figure 1**a, b, the voltage losses can be categorized into three contributions based on the SQ limit:[44]

$$\Delta V_{OC} = E_g/q - V_{OC} = \left(E_g/q - V_{OC}^{SQ}\right) + \left(V_{OC}^{SQ} - V_{OC}^{rad}\right) + \left(V_{OC}^{rad} - V_{OC}\right) = \Delta V_1 + \Delta V_2 + \Delta V_3 \,. \quad (1)$$

where E_g is the gap of the material with lower gap in the blend, no matter whether it is a donor or an acceptor material. V_{OC}^{SQ} in the equation is the maximum voltage based on the Shockley-Queisser limit, where the *EQE* is assumed to be a step-function, *i.e.*, 1 above the gap and 0 below the gap (**Figure 1**a). In the SQ limit, V_{OC}^{SQ} follows[44]

$$V_{OC}^{SQ} = \frac{kT}{q}\ln\left(\frac{J_{SC}^{SQ}}{J_0^{SQ}} + 1\right) \cong \frac{kT}{q}\ln\left(\frac{q.\int_{E_g}^{+\infty} \emptyset_{AM1.5G}(E).\mathrm{d}E}{q.\int_{E_g}^{+\infty} \emptyset_{BB}(E).\mathrm{d}E}\right) \,. \quad (2)$$

V_{OC}^{rad} is the voltage where the radiative recombination in the device is the sole loss mechanism but where the solar cell quantum efficiency is arbitrarily shaped (**Figure 1**b), and follows from[44]

$$V_{OC}^{rad} = \frac{kT}{q}\ln\left(\frac{J_{SC}}{J_0^{rad}} + 1\right) \cong \frac{kT}{q}\ln\left(\frac{q.\int_0^{+\infty} EQE(E).\emptyset_{AM1,5G}(E).dE}{q.\int_0^{+\infty} EQE(E).\emptyset_{BB}(E).dE}\right) \,. \quad (3)$$

Here, k is Boltzmann's constant, T is the temperature of the solar cell (T = 300 K is used in this paper), q is elementary charge and $\emptyset_{BB}(E)$ is the black body spectrum at the temperature T of the solar cell.

In Equation 2, the V_{OC}^{SQ} is only determined by E_g assuming a given illumination spectrum and temperature. In contrast, in Equation 3, V_{OC}^{rad} is determined independently of any definition of E_g, and it is a constant for a given EQE spectrum. Thus, different E_g definitions affect the determination of ΔV_1 and ΔV_2, but not that of ΔV_3 (refer to Equation 1).

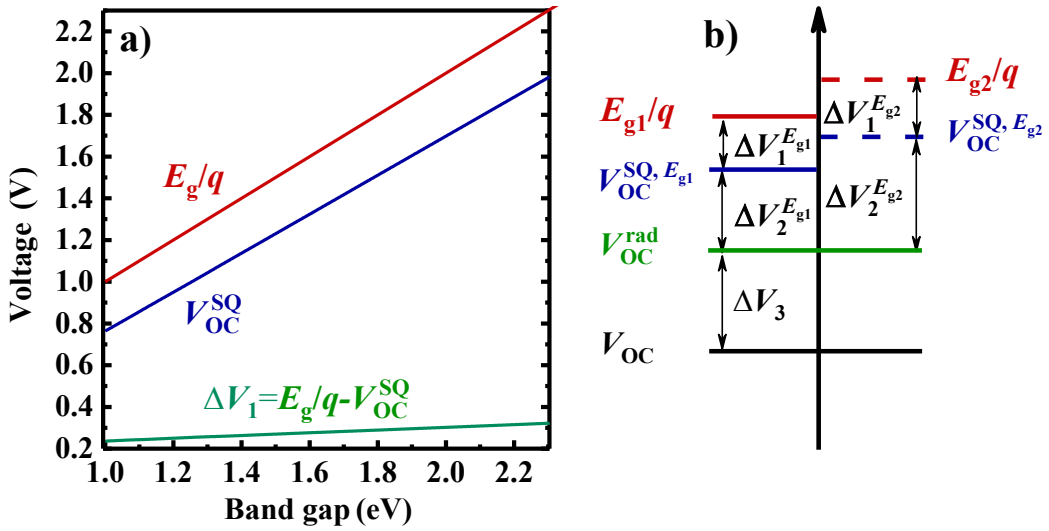

Figure 3. a) The E_g/q (red line), V_{OC}^{SQ} (blue line) and $E_g - V_{OC}^{SQ}$ (green line) plotted as a function of the band gap E_g. The range of the band gap is from 1.0 eV to 2.3 eV, which is suitable for most common OSC materials. b) The variation of ΔV_1 and ΔV_2 due to different E_g values (E_{g1} and E_{g2}) from different definitions.

We further proceed to understand how different definitions for the optical gap affect the quantification of ΔV_1 and ΔV_2. ΔV_1 results from unavoidable radiative recombination, and it normally ranges from ~0.2 to ~0.3 eV, depending on the E_g. **Figure 3**a presents plots of V_{OC}^{SQ} and E_g/q as functions of E_g according to Equation 2. Since the steepness difference between these two

curves is small, their difference ΔV_1 is small when different E_g definitions are used, as shown in the bottom line of **Figure 3**a. The variation of ΔV_2 is equal to the variation of V_{OC}^{SQ} (**Figure 3**b). In other words, different E_g definitions mainly affect the value of ΔV_2.

As shown in **Figure 1**a, b and **Figure 3**b, ΔV_2 is the difference between V_{OC}^{SQ} and V_{OC}^{rad}, which results from the non-stepfunction like absorptance or *EQE* of the real-world devices. The ΔV_2 can be further categorized into two contributions:[63]

$$\Delta V_2 = \frac{kT}{q}\ln\left(\frac{J_{SC}^{SQ}}{J_0^{SQ}}\right) - \frac{kT}{q}\ln\left(\frac{J_{SC}}{J_0^{rad}}\right) = \frac{kT}{q}\ln\left(\frac{J_{SC}^{SQ}}{J_{SC}}\right) + \frac{kT}{q}\ln\left(\frac{J_0^{rad}}{J_0^{SQ}}\right) = \Delta V_2^{SC} + \Delta V_2^{0} . \quad (4)$$

The first loss term, ΔV_2^{SC}, is due to the difference between the real-world short-circuit current density (J_{SC}) and the ideal one in the SQ limit (J_{SC}^{SQ}), and the contribution from ΔV_2^{SC} to the total voltage losses is small for most solar cells. The second loss term, ΔV_2^{0}, is due to the shift of the luminescent emission with respect to a determined E_g (**Figure 1**a, b), leading to a J_0^{rad} that can be orders of magnitude larger that J_0^{SQ}.[63] Thus the ΔV_2 is mostly affected by ΔV_2^{0}.

As reported, ΔV_2^{0} in OSCs particularly exhibits much larger values than that in other solar cell technologies, because of the existence of the strongly red-shifted charge transfer (CT) states.[63] Nowadays, non-fullerene acceptors (mainly small molecules) are developing quickly; in particular, highly efficient charge generation is still available when the driving force is reduced to nearly ~0 eV.[64] This suggests that a negligibly small energy difference between the CT states and the singlet states can be sufficient for charge separation, although it does not yet explain how to achieve efficient charge separation for low offsets.[44, 54-55] In these cases, no red-shifted CT absorption tail and electroluminescence can be observed, resulting in the significantly reduced ΔV_2^{0} and leading to reduced total open-circuit voltage losses ΔV_{OC}.[44, 55]

In order to accurately evaluate ΔV_2 (and ΔV_2^0), reproducible and consensus determination methods of E_g are required. In the following sections, we will briefly introduce several E_g determination methods, which have been frequently employed in the literature.

3. Extracting the E_g by the onset of the absorption (or *EQE*) spectrum

The most commonly used method of determining the optical gap for voltage loss calculations is to take E_g as depicted in **Figure 2**a, by the intersection of the linear fitting curve of the absorption spectrum and the abscissa axis (or the tangent of absorption tail).[31-32, 34, 65] This approach is subjective and results are not well reproducible, especially when there is no strict linear region in the absorption edge or when the light scattering is very significant for the absorption tail, which is often the case for spin-coated organic films.[66] Furthermore, a physical base for this method is absent.[56]

Note that the absorptance onset of the material with the smallest E_g can be significantly shifted after blending with other materials. For example, Ran et al. [65] reported a case, where the absorption edge of blend film demonstrates a red shift as large as ~70 meV, compared with that of the neat film (**Figure 4**). They attributed the red-shifted absorptance edge to the changes in structure and/or the surrounding environment of the polymer in the blend film. Therefore, in the cases where morphology effects induce obvious E_g variations, it is necessary to employ the spectra of blend films rather than that of neat films to determine E_g.

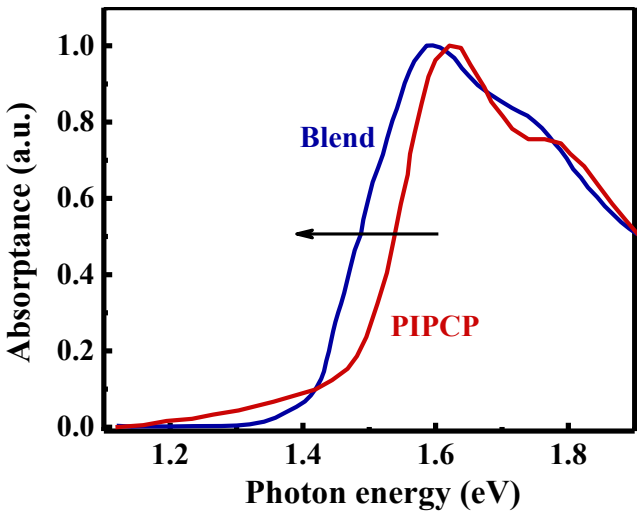

Figure 4. Absorption spectra of blend PIPCP:$PC_{61}BM$ films (blue curve) and neat PIPCP films (red curve). The absorption onset of the blend films is red-shifted by ~70 meV compared with that of neat PIPCP films. Reproduced with permission.[65] Copyright 2015, Wiley-VCH.

In addition, using the absorption onset usually yields smaller values for E_g as compared with other determination methods, and hence leads to lower voltage losses. For example, the E_g of neat (2,2′-((2*Z*,2′*Z*)-(((4,4,9-tris(4-hexylphenyl)-9-(4-pentylphenyl)-4,9-dihydro-*s*-indaceno[1,2-*b*:5,6-*b* dithiophene-2,7-diyl)bis(4-((2-ethylhexyl)oxy)thiophene-5,2-diyl))bis(methanylylidene))bis(5,6-dichloro-3-oxo-2,3-dihydro-1*H*-indene-2,1-diylidene))dimalononitrile) (IEICO-4Cl) films determined from the absorption onset results in a value of ~1.25 eV.[33] Based on the methods demonstrated in Section 2, we employ this value to quantify the voltage losses of the device based on poly[(2,6-(4,8-bis(5-(2-ethylhexyl)thiophen-2-yl)-benzo[1,2-b:4,5-b']dithiophene))-alt-(5,5-(1',3'-di-2-thienyl-5',7'-bis(2-ethylhexyl)benzo[1',2'-c:4',5'-c']dithiophene-4,8-dione))] (PBDB-T):IEICO-4Cl. The quantification results are as presented in **Table 1**.

Table 1. Quantification of voltage losses of the device based on PBDB-T:IEICO-4Cl.

Materials	E_{opt}/q [V]	V_{OC}^{SQ} [V]	V_{OC}^{rad} [V]	ΔV_1 [V]	ΔV_2 [V]	ΔV_2^{SC} [V]	ΔV_2^0 [V]	ΔV_3 [V]	ΔV_{OC} [V]
PBDB-T:IEICO-4Cl	1.25	0.99	1.02	0.25	-0.03	0.02	-0.05	0.29	0.51

As shown in **Table 1**, the theoretical maximum open-circuit voltage ($V_{\mathrm{OC}}^{\mathrm{SQ}}$) in the SQ limit for a device based on the material with an E_{g} of 1.25 eV is ~0.99 V. However, the radiative open-circuit voltage ($V_{\mathrm{OC}}^{\mathrm{rad}}$) of the device based on PBDB-T:IEICO-4Cl is ~1.02V, which is larger than the $V_{\mathrm{OC}}^{\mathrm{SQ}}$, corresponding to a negative ΔV_2 of ~0.03 eV. As discussed in section 2, ΔV_2 is caused by the fact that the *EQE* curve of a practical solar cell cannot be a step-function assumed in the SQ limit (**Figure 1**b), and it is mainly caused by the radiative recombination loss below E_{g} (ΔV_2^0). The negative value of ΔV_2 suggests that the definition of E_{g} from the absorption onset is not helpful at all in the context of a voltage loss analysis as introduced in section 2. However, recent papers claiming to obtain small voltage losses, mostly determined the E_{g} from the onset of the absorption spectrum, underestimating the E_{g} leading to a smaller calculated voltage losses.[54]

4. Extracting E_g by the intersection between the normalized absorption and emission spectra of the organic material in the solid film

The estimation of E_{g} by the onset of the absorption spectrum is rather arbitrary and ill-defined. An alternative and more well-defined estimation of E_{g} uses the intersection of the normalized absorption and emission spectra (**Figure 2**b).[54, 56, 66-67] **Figure 1d** depicts the optical transitions from the ground states to the singlet states in bulk-heterojunction OSCs. The maximum absorption

is obtained when the vertical electronic transitions occur from the initial ground state (GS) to the most probable excited singlet state. Relaxation subsequently occurs to the lowest excited singlet state with relaxed energy λ_{abs}. Likewise, the vertical transitions occur from the lowest excited singlet state to the most probable vibrational ground state, forming the maximum luminescence. Subsequently, relaxation occurs to the initial ground state with relaxed energy λ_{fl}. The corresponding vertical transition energies for absorption and luminescence are given by

$$E_{\mathrm{max,abs}} = E_{0-0} + \lambda_{\mathrm{abs}} \tag{5}$$

and

$$E_{\mathrm{max,fl}} = E_{0-0} - \lambda_{\mathrm{fl}}, \tag{6}$$

where λ_{abs} and λ_{fl} are the relaxed energies in the absorption and emission processes, respectively. $E_{\mathrm{max,abs}}$ is the energy at maximum absorption, and $E_{\mathrm{max,fl}}$ is the energy at maximum emission. E_{0-0} is the energy from the initial ground state to the lowest singlet excited state, which is defined as the optical gap of the material.

When the absorption and emission spectra in their overlap area are approximately symmetric (valid for most organic semiconductors), E_{0-0} can be determined as the energy at the intersection of the normalized absorptance and emission spectra. Determining E_g at the intersection of absorption and emission is physically motivated and well reproducible. A similar method is used to define the optical gap of charge transfer states (or the CT state energy E_{CT}) by the absorptance and emission of charge transfer states in OSCs. [37, 54, 56]

Similar to the first E_{g} definition method, we need to use the absorptance and emission spectra of blend films in the case where the absorption onset is shifted in the blend films. **Figure 5** depicts

the shifted absorptance and photoluminescence (PL) onset of IEICO-4Cl after blending with poly[[2,6′-4,8-di(5-ethylhexylthienyl)benzo[1,2-b;3,3-b]dithiophene][3-fluoro-2[(2-ethylhexyl)carbonyl]thieno[3,4-b]thiophenediyl]] (PTB7-Th).

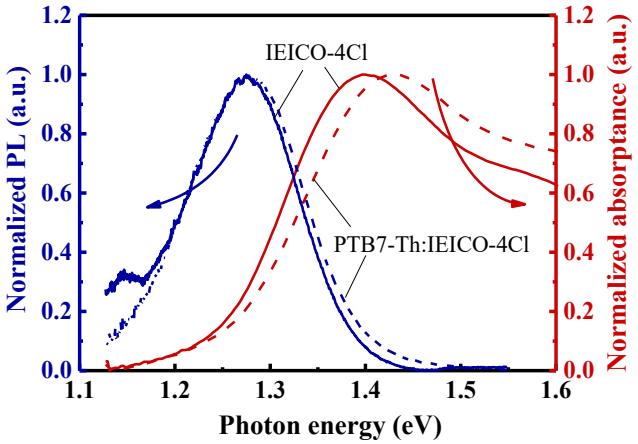

Figure 5. The absorption spectra (red lines) and PL spectra (blue lines) of IEICO-4Cl (solid lines) and PTB7-Th:IEICO-4Cl (dashed lines). The PL spectrum edge of blend films blue shifts by ~10 meV and the absorption edge of blend film blue shifts by ~20 meV in relative to that of the neat film.

We summarize the E_g values of commonly used OSC materials, obtained from the intersection of absorption and PL spectra of films, in **Table 2**.

Table 2. E_g values extracted from the normalized absorption and PL spectra of neat films of a range of organic semiconductors. The chemical structures of the materials are given in the Ref.

Materials	E_{0-0} [eV]	Ref.	Materials	E_{0-0} [eV]	Ref.
PTB7-Th	1.67	[68]	IDTIDSe-IC	1.65	[69]
PBDB-T	1.88	[30]	IT-M	1.67	[31]
PDPP3T	1.41	[70]	IEICO	1.45	[32]
TQ1	1.81	[71]	O-IDTBR	1.71	[72]
PffBT4T-2DT	1.71	[55]	IEICO-4F	1.36	[73]
P3TEA	1.72	[44]	IEICO-4Cl	1.33	[33]
PNOz4T	1.58	[74]	ATT-1	1.63	[75]
ITIC	1.68	[30]	N2200	1.54	[76]

5. Extracting the E_g from the *EQE* spectrum of the device

Some recent reports also proposed to determine the E_g from the *EQE* spectrum.[54, 56] Determining E_g from the *EQE* spectrum has its own advantages, such as being easily accessible and excluding influences of morphological effects. In contrast to absorption and emission of films, the *EQE* spectrum is not only correlated to the internal properties of absorbing materials, but also dependent on the device structure (the thickness of the active layer, the optical properties of interlayers and electrodes) because interference effects can slightly change the shape of *EQE* spectrum.[54] Hence, the *EQE* spectrum represents an external property of a complete solar cell. In the following part, we will introduce two E_g determination methods based on the *EQE* spectrum.

A recent method proposed by Vandewal et al. for evaluating the voltage losses is to use the crossing point of the extrapolated line of the *EQE* edge and the horizontal tangent of the *EQE* peak, denoted as E_g^{edge}.[54, 56] In the SQ model, where *EQE* is a step-function, the E_g^{edge} would coincide with E_g. In the real-world PV devices, where the *EQE* spectrum is not a step-function, the E_{edge} metric takes into account the abruptness of the *EQE* edge. For the voltage loss calculation, this method reflects that fact that very good photovoltaic devices should have sharp absorption edges, where E_g^{edge} is close to the absorption onset as defined in **Figure 2**a. **Figure 2**c illustrates this definition of E_g^{edge} as determined from an *EQE* spectrum.

Based on the idea that any experimental absorptance or *EQE* can be interpreted as a superposition of a distribution of SQ-type step-functions with different band gap energies, Rau et al. proposed a photovoltaic band-gap energy (E_g^{PV}), which can be obtained from the *EQE* edge directly.[63, 77] In the SQ model, the absorption or *EQE* spectrum as a function of photon energy is an ideal step-function (**Figure 1**a), which cannot exist in real-world OSCs (**Figure 1**b). If we

interpret the *EQE* as consisting of a distribution of step-functions with a step at E_g^{SQ} having a certain probability distribution $P(E_g^{SQ})$, we find that this probability distribution can be obtained from the derivative *dEQE*/*dE*. There are different ways of how to assign a "band gap" to the distribution *P*(*E*) = *dEQE*/*dE*. One option is to use[63]

$$E_g^{PV} = \frac{\int_a^b E_g.P(E_g).dE_g}{\int_a^b P(E_g).dE_g}. \quad (7)$$

Here, the integral boundaries a and b are selected where $P(a) = P(b) = 0.5\max[P(E_g)]$ (**Figure 2**d). The selection of integral boundaries serves to exclude the influence of noisy data and negative value of $P(E_g)$, and is not physically motivated.[63] While the factor 0.5 in the in the choice of a and b is fairly arbitrary, slightly different choices would not strongly affect the result except for very noisy data. The determination of E_g from *EQE* spectra is relatively easy to implement as well as physically motivated and allows comparison of the ΔV_{OC} of devices in previously reported papers.

6. Voltage losses and efficiency prediction

In 2006, Scharber et al. proposed a simple guideline for the efficiency potential of polymer: fullerene based single junction OSCs. In their guideline, the open-circuit voltage V_{OC} is empirically given by interfacial energy gap (divided by q) minus 0.3V.[78] Scharber et al calculated the short-circuit current density J_{SC} based on a step-function *EQE* of 65% above E_g and 0 below E_g. The model of ref.[78] allows us to predict the efficiency potential from the band gap and the LUMO offset of the materials in a rather simple and empirical way. Subsequently, efficiency predictions similar to Scharber's methods were performed, and the open-circuit voltage losses, rather than

LUMO offset, were employed.[55, 79] For a long time, the community believed that the EQE_{max} is correlated with the voltage losses, especially in fullerene based OSCs, as empirically summarized by Li et al in 2015.[62] The underlying reason for the dependence of EQE_{max} on ΔV_{OC} was believed to be the driving force for charge separation. A combination of the Scharber approach with the empirical relation between EQE_{max} and open-circuit voltage loss was used by Baran et al. for efficiency potential estimations.[55, 80]

However, the situation has now changed, with a range of new systems demonstrating efficient charge separation in spite of negligible energetic offsets between the donor and acceptor materials, leading to the small ΔV_{OC}.[44, 64, 72, 81-83] These recent new advances challenge the traditional belief that a sufficiently large energetic offset is required for efficient charge separation. We summarize the EQE_{max} and ΔV_{OC} values reported in literature, as shown in Table 3, and plot the EQE_{max} as a function of ΔV_{OC} in **Figure 6**a-c. The E_g values are defined from the *EQE* onset (E_g^{onset}), derivatives of the *EQE* (E_g^{PV}), and the crossing point between the extrapolated line of the *EQE* edge and horizontal tangent of the local peak (E_g^{edge}), respectively.

Table 3. Summarized parameters of representative devices in literature. The chemical structures of these materials are given in the references.

Materials	V_{OC} [V]	EQE_{max} [%]	E_g^{onset} [eV]	ΔV_{OC}^{onset} [V]	E_g^{PV} [eV]	ΔV_{OC}^{PV} [V]	E_g^{edge} [eV]	ΔV_{OC}^{edge} [V]	Ref.
PFBDBT-T:C8-ITIC	0.93	86.8	1.53	0.60	1.57	0.64	1.67	0.74	[25]
PBDBT-T:C8-ITIC	0.86	84.0	1.52	0.66	1.59	0.73	1.66	0.80	[25]
PBDB-T:ITIC	0.91	78.5	1.59	0.68	1.65	0.74	1.72	0.81	[30]
PBDTT-E-T:IEICO	0.82	68.4	1.38	0.56	1.44	0.62	1.50	0.68	[32]
PBDB-T:IEICO-4Cl	0.74	64.1	1.25	0.51	1.31	0.57	1.36	0.62	[33]
J52:IEICO-4Cl	0.70	74.2	1.25	0.55	1.31	0.61	1.36	0.66	[33]
PTB7-Th:IEICO-4Cl	0.73	72.3	1.25	0.52	1.31	0.58	1.36	0.63	[33]

P3TEA:SF-PDI2	1.11	65.4	1.67	0.56	1.73	0.62	1.78	0.67	[44]
6T/rubrene(8nm)/SubNc/SubPc	1.16	79.5	1.67	0.51	1.69	0.53	1.75	0.59	[54]
PffBT4T-2DT:O-IDTBR	1.07	56.5	1.61	0.54	1.69	0.62	1.73	0.66	[55]
PTB7-Th:$PC_{71}BM$	0.82	80.0	1.58	0.76	1.64	0.82	1.70	0.88	[68]
PBDB-T:$PC_{71}BM$	0.86	73.2	1.77	0.91	1.86	1.00	1.95	1.09	[84]
PIPCP:$PC_{61}BM$	0.86	61.8	1.42	0.56	1.46	0.60	1.54	0.68	[85]
DPPEZnP-THE:$PC_{61}BM$	0.78	66.3	1.42	0.64	1.49	0.71	1.55	0.77	[86]
PDPP2TzDTP:$PC_{71}BM$	0.69	51.3	1.31	0.62	1.36	0.67	1.41	0.72	[62]
DR3TSBDT:DTBTF	1.15	43.1	1.76	0.61	1.83	0.68	1.91	0.76	[87]
PNOz4T:$PC_{61}BM$	0.98	68.3	1.51	0.53	1.56	0.58	1.61	0.63	[74]
P3HT:SF(DPPB)4	1.14	47.6	1.80	0.66	1.84	0.70	1.88	0.74	[88]
PIDTT-TID:$PC_{71}BM$	1.00	69.3	1.50	0.50	1.59	0.59	1.70	0.70	[89]
PDCBT-2F:IT-M	1.13	49.4	1.62	0.49	1.68	0.55	1.74	0.61	[90]
J61:ITIC	0.89	77.7	1.58	0.69	1.65	0.76	1.73	0.84	[91]
DRCN5T:TPH	1.04	55.6	1.62	0.58	1.69	0.65	1.75	0.71	[92]
PTB7-th:IDT-IC	0.83	54.1	1.60	0.77	1.69	0.86	1.76	0.93	[93]
PTB7-th:IDTIDT-IC	0.84	66.6	1.55	0.71	1.61	0.77	1.68	0.84	[93]
PTB7-th:PDI-2DTT	1.05	69.7	1.59	0.54	1.64	0.59	1.70	0.65	[94]
TQ1:$PC_{71}BM$	0.91	61.8	1.72	0.81	1.85	0.94	1.99	1.08	[71]
PDPP3T:$PC_{71}BM$	0.65	45.0	1.32	0.67	1.36	0.71	1.41	0.76	[70]
PTB7-Th:IEICO-4F	0.74	77.9	1.27	0.53	1.32	0.58	1.38	0.64	[73]
J52-2F:IT-M	0.95	82.1	1.59	0.64	1.67	0.72	1.75	0.80	[95]
PvBDTTAZ:O-IDTBR	1.08	71.0	1.61	0.53	1.67	0.59	1.73	0.65	[72]
J51:IDTIDSe-IC	0.91	61.1	1.54	0.63	1.59	0.68	1.64	0.73	[69]
PDBDT-TDZ:ITIC	1.10	80.0	1.58	0.48	1.64	0.54	1.70	0.60	[81]

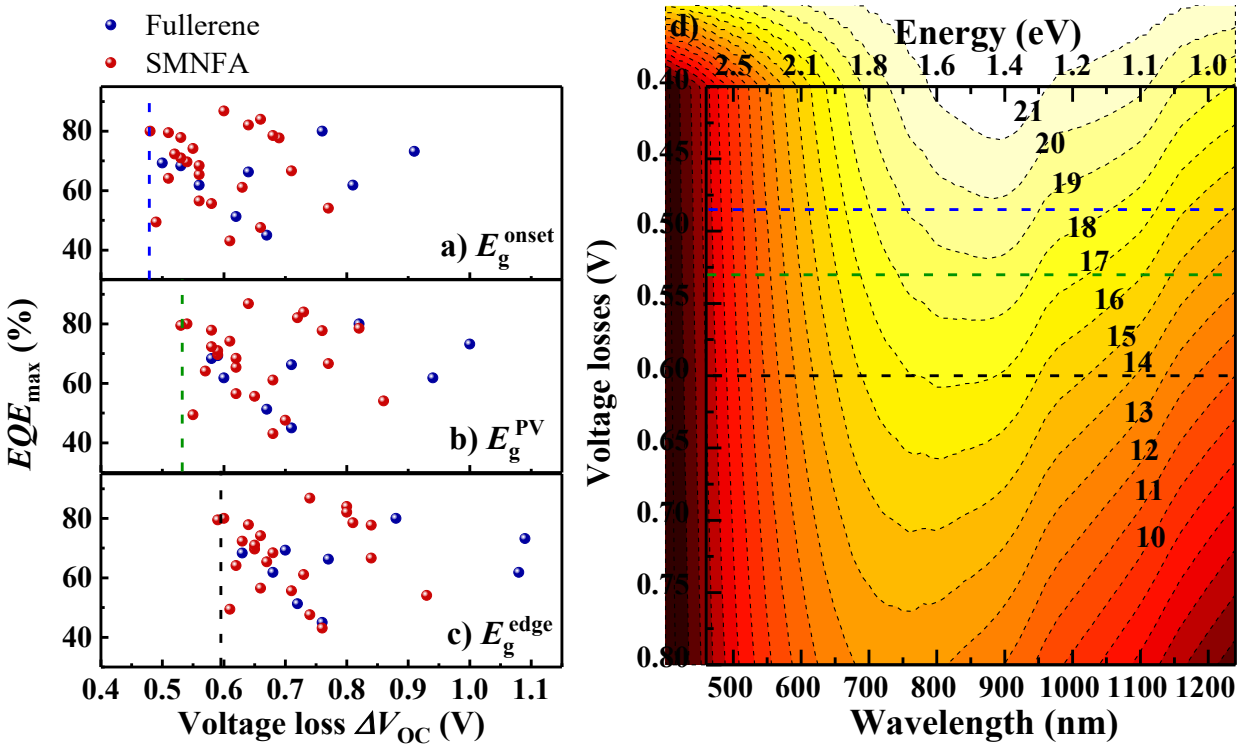

Figure 6. The EQE_{max} versus ΔV_{OC} of the devices based on fullerene acceptors (blue spheres) and small molecular non-fullerene acceptors (SMNFA) (red spheres), and the ΔV_{OC} is calculated from different E_g definitions: a) *EQE* onset (E_g^{onset}), b) derivative of *EQE* (E_g^{PV}) and c) crossing point of extrapolated line of the *EQE* edge and c) horizontal tangent of the local peak (E_g^{edge}). The data sources are as depicted in **Table 3**. d) The efficiency prediction as a function of optical gap taken from ref. [79], where the EQE_{max} was assumed to be independent of ΔV_{OC}. The dashed lines indicate the smallest ΔV_{OC} (depending on different E_g definitions) achieved by the OSC community so far. Part d) reproduced with permission.[79] Copyright 2018, Macmillan Publishers ltd.

As shown in **Figure 6**a-c, there is no clear tendency showing that the EQE_{max} is dependent on the ΔV_{OC}. For all three E_g definitions, the quantum efficiency in **Figure 6**a-c can remain high when ΔV_{OC} approaches ~0.6 V. This conclusion leads us to **Figure 6**d, a recent efficiency prediction where the *EQE* is assumed to be a constant (85%), independent of ΔV_{OC}.[79] With a given E_g, **Figure 6**d is supposed to provide us with information concerning what the maximum efficiency could be and whether the ΔV_{OC} is already small enough (and hence what the direction is for future optimization of the devices). However, as we can see from the figure, different E_g definitions

certainly give us different conclusions, indicating the importance to choose a proper definition so that the prediction in **Figure 6**d can help us to further optimize the device. By its definition, E_g^{onset} takes the point where the absorption is zero. The prediction in **Figure 6**d (and also any other efficiency prediction) uses a constant *EQE* value above E_g, indicating that the definition of E_g^{onset} is not useful for the prediction. Based on this consideration, **Figure 6**d predicts that a PCE of ~ 17%-18% (dependent on the definition of E_g^{PV} or E_g^{edge}, indicated as black and green dash lines in the figure) can be achieved with the smallest ΔV_{OC} currently achievable in literature, if other parameters are optimized i.e., ~85% *EQE* value over a wide wavelength range and ~75% *FF*.

7. Conclusion

In summary, we analyzed how each part of the voltage loss calculation is influenced by the variation of E_g values due to different E_g determination methods. We introduced different E_g determination methods for OSCs and discussed their advantages and disadvantages. The E_g determined from the onset of either absorptance or *EQE* spectra bears no physical meaning and leads to ill-defined voltage losses. In addition, the E_g value determined in this way is not relevant for efficiency prediction. The E_g determined from the crossing point between absorption and emission spectra does have a clear physical meaning, although not all groups report these spectra. At the same time, we note that this approach could be challenging when E_g of the single components changes significantly in the donor-acceptor blend due to morphological effects. The concepts of E_g^{edge} and E_g^{PV}, which can be directly determined by the *EQE* spectrum without any additional optical measurements, bridges the SQ limit and real-world photovoltaic devices, providing straightforward and useful definitions. Based on the definitions of E_g^{edge} or E_g^{PV}, the

voltage losses of state-of-the-art OSCs are not much less than 0.6 V, leading to a prediction of a realistic efficiency upper limit of ~ 18 % for single cells. We will therefore need to further decrease the voltage losses if we want to improve the efficiency of OSCs to the level of high-efficiency inorganic and perovskite solar cells. We hope that this paper helps the OSC community to use the proper E_g definitions in the future so that we can make the voltage losses comparable.

Acknowledgements

The authors acknowledge the support from the Swedish Research Council VR (2017-00744), the Swedish Energy Agency Energimyndigheten (2016-010174), the Swedish Government Strategic Research Area in Materials Science on Functional Materials at Linköping University (Faculty Grant No. SFO-Mat-LiU #2009-00971), the DFG (Grant KI-1571/2-1), the Knut Alice Wallenberg Foundation (KAW), and the China Scholarship Council.

Reference

[1] C. W. Tang, *Appl. Phys. Lett.* **1986**, *48*, 183.

[2] M. Muntwiler, Q. Yang, W. A. Tisdale, X. Y. Zhu, *Phys. Rev. Lett.* **2008**, *101*, 196403.

[3] C. H. Peters, I. T. Sachs-Quintana, W. R. Mateker, T. Heumueller, J. Rivnay, R. Noriega, Z. M. Beiley, E. T. Hoke, A. Salleo, M. D. McGehee, *Adv. Mater.* **2012**, *24*, 663.

[4] S. M. Falke, C. A. Rozzi, D. Brida, M. Maiuri, M. Amato, E. Sommer, A. De Sio, A. Rubio, G. Cerullo, E. Molinari, *Science* **2014**, *344*, 1001.

[5] N. A. Ran, S. Roland, J. A. Love, V. Savikhin, C. J. Takacs, Y.-T. Fu, H. Li, V. Coropceanu, X. Liu, J.-L. Brédas, G. C. Bazan, M. F. Toney, D. Neher, T.-Q. Nguyen, *Nat. Commun.* **2017**, *8*, 79.

[6] A. C. Jakowetz, M. L. Böhm, A. Sadhanala, S. Huettner, A. Rao, R. H. Friend, *Nat. Mater.* **2017**, *16*, 551.

[7] F. Gao, W. Tress, J. Wang, O. Inganäs, *Phys. Rev. Lett.* **2015**, *114*, 128701.

[8] X. Che, Y. Li, Y. Qu, S. R. Forrest, *Nat. Energy* **2018**, *3*, 422.

[9] G. Yu, J. Gao, J. C. Hummelen, F. Wudl, A. J. Heeger, *Science* **1995**, *270*, 1789.

[10] A. A. Bakulin, A. Rao, V. G. Pavelyev, P. H. van Loosdrecht, M. S. Pshenichnikov, D. Niedzialek, J. Cornil, D. Beljonne, R. H. Friend, *Science* **2012**, *335*, 1340.

[11] S. M. Menke, A. Cheminal, P. Conaghan, N. A. Ran, N. C. Greehnam, G. C. Bazan, T.-Q. Nguyen, A. Rao, R. H. Friend, *Nat. Commun.* **2018**, *9*, 277.

[12] Y. Liang, Z. Xu, J. Xia, S.-T. Tsai, Y. Wu, G. Li, C. Ray, L. Yu, *Adv. Mater.* **2010**, *22*, E135.

[13] Z. He, C. Zhong, X. Huang, W.-Y. Wong, H. Wu, L. Chen, S. Su, Y. Cao, *Adv. Mater.* **2011**, *23*, 4636.

[14] Y. Sun, G. C. Welch, W. L. Leong, C. J. Takacs, G. C. Bazan, A. J. Heeger, *Nat. Mater.* **2011**, *11*, 44.

[15] Z. He, C. Zhong, S. Su, M. Xu, H. Wu, Y. Cao, *Nat. Photon.* **2012**, *6*, 591.

[16] Q. Zhang, B. Kan, F. Liu, G. Long, X. Wan, X. Chen, Y. Zuo, W. Ni, H. Zhang, M. Li, Z. Hu, F. Huang, Y. Cao, Z. Liang, M. Zhang, T. P. Russell, Y. Chen, *Nat. Photon.* **2014**, *9*, 35.

[17] M. Qian, R. Zhang, J. Hao, W. Zhang, Q. Zhang, J. Wang, Y. Tao, S. Chen, J. Fang, W. Huang, *Adv. Mater.* **2015**, *27*, 3546.

[18] D. Baran, R. S. Ashraf, D. A. Hanifi, M. Abdelsamie, N. Gasparini, J. A. Röhr, S. Holliday, A. Wadsworth, S. Lockett, M. Neophytou, C. J. M. Emmott, J. Nelson, C. J. Brabec, A. Amassian, A. Salleo, T. Kirchartz, J. R. Durrant, I. McCulloch, *Nat. Mater.* **2016**, *16*, 363.

[19] B. Kan, H. Feng, X. Wan, F. Liu, X. Ke, Y. Wang, Y. Wang, H. Zhang, C. Li, J. Hou, Y. Chen, *J. Am. Chem. Soc.* **2017**, *139*, 4929.

[20] T. Liu, X. Pan, X. Meng, Y. Liu, D. Wei, W. Ma, L. Huo, X. Sun, T. H. Lee, M. Huang, H. Choi, J. Y. Kim, W. C. H. Choy, Y. Sun, *Adv. Mater.* **2017**, *29,* 1604251.

[21] C. Sun, F. Pan, H. Bin, J. Zhang, L. Xue, B. Qiu, Z. Wei, Z.-G. Zhang, Y. Li, *Nat. Commun.* **2018**, *9*, 743.

[22] L. Yang, W. Gu, L. Lv, Y. Chen, Y. Yang, P. Ye, J. Wu, L. Hong, A. Peng, H. Huang, *Angew. Chem., Int. Ed.* **2018**, *57*, 1096.

[23] Z. Xiao, X. Jia, L. Ding, *Sci. Bull.* **2017**, *62*, 1562.

[24] W. Zhao, S. Li, H. Yao, S. Zhang, Y. Zhang, B. Yang, J. Hou, *J. Am. Chem. Soc.* **2017**, 139, 7148.

[25] Z. Fei, F. D. Eisner, X. Jiao, M. Azzouzi, J. A. Rohr, Y. Han, M. Shahid, A. S. R. Chesman, C. D. Easton, C. R. McNeill, T. D. Anthopoulos, J. Nelson, M. Heeney, *Adv. Mater.* **2018**, *30*.

[26] S. Zhang, Y. Qin, J. Zhu, J. Hou, *Adv. Mater.*, DOI: 10.1002/adma.201800868.

[27] H. Li, Z. Xiao, L. Ding, J. Wang, *Sci. Bull.* **2018**, *63*, 340.

[28] Y. Lin, J. Wang, Z. G. Zhang, H. Bai, Y. Li, D. Zhu, X. Zhan, *Adv. Mater.* **2015**, *27*, 1170.

[29] Y. Lin, Z.-G. Zhang, H. Bai, J. Wang, Y. Yao, Y. Li, D. Zhu, X. Zhan, *Energy Environ. Sci.* **2015**, *8*, 610.

[30] W. Zhao, D. Qian, S. Zhang, S. Li, O. Inganas, F. Gao, J. Hou, *Adv. Mater.* **2016**, *28*, 4734.

[31] S. Li, L. Ye, W. Zhao, S. Zhang, S. Mukherjee, H. Ade, J. Hou, *Adv. Mater.* **2016**, *28*, 9423.

[32] H. Yao, Y. Chen, Y. Qin, R. Yu, Y. Cui, B. Yang, S. Li, K. Zhang, J. Hou, *Adv. Mater.* **2016**, *28*, 8283.

[33] Y. Cui, C. Yang, H. Yao, J. Zhu, Y. Wang, G. Jia, F. Gao, J. Hou, *Adv. Mater.* **2017**, *29*, 1703080.

[34] H. Yao, L. Ye, J. Hou, B. Jang, G. Han, Y. Cui, G. M. Su, C. Wang, B. Gao, R. Yu, H. Zhang, Y. Yi, H. Y. Woo, H. Ade, J. Hou, *Adv. Mater.* **2017**, *29*, 1700254.

[35] K. Vandewal, A. Gadisa, W. D. Oosterbaan, S. Bertho, F. Banishoeib, I. Van Severen, L. Lutsen, T. J. Cleij, D. Vanderzande, J. V. Manca, *Adv. Funct. Mater.* **2008**, *18*, 2064.

[36] K. Vandewal, K. Tvingstedt, A. Gadisa, O. Inganas, J. V. Manca, *Nat. Mater.* **2009**, *8*, 904.

[37] K. Vandewal, K. Tvingstedt, A. Gadisa, O. Inganäs, J. V. Manca, *Phys. Rev. B* **2010**, *81*, 125204.

[38] J. Benduhn, F. Piersimoni, G. Londi, A. Kirch, J. Widmer, C. Koerner, D. Beljonne, D. Neher, D. Spoltore, K. Vandewal, *Adv. Energy Mater.* **2017,** *7***,** 1700855.

[39] C. J. Brabec, A. Cravino, D. Meissner, N. S. Sariciftci, T. Fromherz, M. T. Rispens, L. Sanchez, J. C. Hummelen, *Adv. Funct. Mater.* **2001**, *11*, 374.

[40] T. M. Burke, S. Sweetnam, K. Vandewal, M. D. McGehee, *Adv. Energy Mater.* **2015**, *5*, 1500123.

[41] A. Gadisa, M. Svensson, M. R. Andersson, O. Inganäs, *Appl. Phys. Lett.* **2004**, *84*, 1609.

[42] Z. Ma, W. Sun, S. Himmelberger, K. Vandewal, Z. Tang, J. Bergqvist, A. Salleo, J. W. Andreasen, O. Inganäs, M. R. Andersson, C. Müller, F. Zhang, E. Wang, *Energy Environ. Sci.* **2014**, *7*, 361.

[43] J. Yao, T. Kirchartz, M. S. Vezie, M. A. Faist, W. Gong, Z. He, H. Wu, J. Troughton, T. Watson, D. Bryant, J. Nelson, *Phys. Rev. Applied* **2015**, *4*, 014020.

[44] J. Liu, S. Chen, D. Qian, B. Gautam, G. Yang, J. Zhao, J. Bergqvist, F. Zhang, W. Ma, H. Ade, O. Inganäs, K. Gundogdu, F. Gao, H. Yan, *Nat. Energy* **2016**, *1*, 16089.

[45] T. Kirchartz, U. Rau, M. Kurth, J. Mattheis, J. H. Werner, *Thin Solid Films* **2007**, *515*, 6238.

[46] U. Rau, *Phys. Rev. B* **2007**, *76*, 085303.

[47] L. J. A. Koster, S. E. Shaheen, J. C. Hummelen, *Adv. Energy Mater.* **2012**, *2*, 1246.

[48] K. Tvingstedt, O. Malinkiewicz, A. Baumann, C. Deibel, H. J. Snaith, V. Dyakonov, H. J. Bolink, *Sci. Rep.* **2014**, *4*, 6071.

[49] M. L. Keshtov, S. A. Kuklin, A. R. Khokhlov, S. N. Osipov, N. A. Radychev, D. Y. Godovskiy, I. O. Konstantinov, F. C. Chen, E. N. Koukaras, G. D. Sharma, *Org. Electro.* **2017**, *46*, 192.

[50] R. Heuvel, J. J. van Franeker, R. A. J. Janssen, *Macromol. Chem. Phys.* **2017**, *218*, 1600502.

[51] W. T. Hadmojo, F. T. A. Wibowo, D. Y. Ryu, I. H. Jung, S. Y. Jang, *ACS Appl. Mater. Interfaces.* **2017**, *9*, 32939.

[52] Z. Du, X. Bao, Y. Li, D. Liu, J. Wang, C. Yang, R. Wimmer, L. W. Städe, R. Yang, D. Yu, *Adv. Energy Mater.*, DOI: 10.1002/aenm.201701471.

[53] D. Yang, H. Sasabe, T. Sano, J. Kido, *ACS Energy Lett.* **2017**, *2*, 2021.

[54] V. C. Nikolis, J. Benduhn, F. Holzmueller, F. Piersimoni, M. Lau, O. Zeika, D. Neher, C. Koerner, D. Spoltore, K. Vandewal, *Adv. Energy Mater*. **2017**, *7*, 1700855.

[55] D. Baran, T. Kirchartz, S. Wheeler, S. Dimitrov, M. Abdelsamie, J. Gorman, R. S. Ashraf, S. Holliday, A. Wadsworth, N. Gasparini, P. Kaienburg, H. Yan, A. Amassian, C. J. Brabec, J. R. Durrant, I. McCulloch, *Energy Environ. Sci.* **2016**, *9*, 3783.

[56] K. Vandewal, J. Benduhn, V. C. Nikolis, *Sustainable Energy & Fuels* **2018**, *2*, 538.

[57] M. H. Cohen, H. Fritzsche, S. R. Ovshinsky, *Phys. Rev. Lett.* **1969**, *22*, 1065.

[58] G. D. Cody, T. Tiedje, B. Abeles, B. Brooks, Y. Goldstein, *Phys. Rev. Lett.* **1981**, *47*, 1480.

[59] A. R. Zanatta, I. Chambouleyron, *Phys. Rev. B* **1996**, *53*, 3833.

[60] C. R. Wronski, S. Lee, M. Hicks, S. Kumar, *Phys. Rev. Lett.* **1989**, *63*, 1420.

[61] B. E. Pieters, H. Stiebig, M. Zeman, R. A. C. M. M. van Swaaij, *J. Appl. Phys.* **2009**, *105*, 044502.

[62] W. Li, K. H. Hendriks, A. Furlan, M. M. Wienk, R. A. Janssen, *J. Am. Chem. Soc.* **2015**, *137*, 2231.

[63] U. Rau, B. Blank, T. C. M. Müller, T. Kirchartz, *Phys. Rev. Applied* **2017**, *7*, 044016.

[64] D. Qian, Z. Zheng, H. Yao, W. Tress, T. Hopper, S. Chen, S. Li, J. Liu, S. Chen, J. Zhang, X. Liu, B. Gao, L. Ouyang, Y. Jin, G. Pozina, I. Buyanova, W. Chen, O. Inganäs, V. Coropceanu, J. Bredas, H. Yan, J. Hou, F. Zhang, A. Bakulin, F. Gao, *Nat. Mater.* **2018**, *17*, 703.

[65] N. A. Ran, J. A. Love, C. J. Takacs, A. Sadhanala, J. K. Beavers, S. D. Collins, Y. Huang, M. Wang, R. H. Friend, G. C. Bazan, T. Q. Nguyen, *Adv. Mater.* **2016**, *28*, 1482.

[66] J. Gierschner, J. Cornil, H. J. Egelhaaf, *Adv. Mater.* **2007**, *19*, 173.

[67] P. Klán, J. Wirz, *Photochemistry of Organic Compounds: From Concepts to Practice,* Wiley, Chichester, UK **2009**.

[68] Z. He, B. Xiao, F. Liu, H. Wu, Y. Yang, S. Xiao, C. Wang, T. P. Russell, Y. Cao, *Nat. Photon.* **2015**, *9*, 174.

[69] Y. Li, D. Qian, L. Zhong, J.-D. Lin, Z.-Q. Jiang, Z.-G. Zhang, Z. Zhang, Y. Li, L.-S. Liao, F. Zhang, *Nano Energy* **2016**, *27*, 430.

[70] F. S. Kim, X. Guo, M. D. Watson, S. A. Jenekhe, *Adv. Mater.* **2010**, *22*, 478.

[71] E. Wang, L. Hou, Z. Wang, S. Hellstrom, F. Zhang, O. Inganas, M. R. Andersson, *Adv. Mater.* **2010**, *22*, 5240.

[72] S. Chen, Y. Liu, L. Zhang, P. C. Y. Chow, Z. Wang, G. Zhang, W. Ma, H. Yan, *J. Am. Chem. Soc.* **2017**, *139*, 6298.

[73] H. Yao, Y. Cui, R. Yu, B. Gao, H. Zhang, J. Hou, *Angew. Chem., Int. Ed.* **2017**, *56*, 3045.

[74] K. Kawashima, Y. Tamai, H. Ohkita, I. Osaka, K. Takimiya, *Nat. Commun.* **2015**, *6*, 10085.

[75] F. Liu, Z. Zhou, C. Zhang, T. Vergote, H. Fan, F. Liu, X. Zhu, *J. Am. Chem. Soc.* **2016**, *138*, 15523.

[76] Z. Li, X. Xu, W. Zhang, X. Meng, W. Ma, A. Yartsev, O. Inganas, M. R. Andersson, R. A. Janssen, E. Wang, *J. Am. Chem. Soc.* **2016**, *138*, 10935.

[77] U. Rau, J. H. Werner, *Appl. Phys. Lett.* **2004**, *84*, 3735.

[78] M. C. Scharber, D. Mühlbacher, M. Koppe, P. Denk, C. Waldauf, A. J. Heeger, C. J. Brabec, *Adv. Mater.* **2006**, *18*, 789.

[79] J. Hou, O. Inganas, R. H. Friend, F. Gao, *Nat. Mater.* **2018**, *17*, 119.

[80] T. Kirchartz, P. Kaienburg, D. Baran, *J. Phys. Chem. C* **2018**, *122*, 5829.

[81] X. Xu, T. Yu, Z. Bi, W. Ma, Y. Li, Q. Peng, *Adv. Mater.* **2018**, *30*.

[82] S. Dai, T. Li, W. Wang, Y. Xiao, T. K. Lau, Z. Li, K. Liu, X. Lu, X. Zhan, *Adv. Mater.* **2018**, 10.1002/adma.201706571.

[83] P. Cheng, G. Li, X. Zhan, Y. Yang, *Nat. Photon.* **2018**, *12*, 131.

[84] D. Qian, L. Ye, M. Zhang, Y. Liang, L. Li, Y. Huang, X. Guo, S. Zhang, Z. a. Tan, J. Hou, *Macromolecules* **2012**, *45*, 9611.

[85] M. Wang, H. Wang, T. Yokoyama, X. Liu, Y. Huang, Y. Zhang, T. Q. Nguyen, S. Aramaki, G. C. Bazan, *J. Am. Chem. Soc.* **2014**, *136*, 12576.

[86] K. Gao, L. Li, T. Lai, L. Xiao, Y. Huang, F. Huang, J. Peng, Y. Cao, F. Liu, T. P. Russell, R. A. Janssen, X. Peng, *J. Am. Chem. Soc.* **2015**, *137*, 7282.

[87] W. Ni, M. Li, B. Kan, F. Liu, X. Wan, Q. Zhang, H. Zhang, T. P. Russell, Y. Chen, *Chem Commun. (Camb.)* **2016**, *52*, 465.

[88] S. Li, W. Liu, M. Shi, J. Mai, T.-K. Lau, J. Wan, X. Lu, C.-Z. Li, H. Chen, *Energy Environ. Sci.* **2016**, *9*, 604.

[89] C. Wang, X. Xu, W. Zhang, J. Bergqvist, Y. Xia, X. Meng, K. Bini, W. Ma, A. Yartsev, K. Vandewal, M. R. Andersson, O. Inganäs, M. Fahlman, E. Wang, *Adv. Energy Mater.* **2016**, *6*, 1600148.

[90] H. Zhang, S. Li, B. Xu, H. Yao, B. Yang, J. Hou, *J. Mater. Chem. A* **2016**, *4*, 18043.

[91] H. Bin, Z. G. Zhang, L. Gao, S. Chen, L. Zhong, L. Xue, C. Yang, Y. Li, *J. Am. Chem. Soc.* **2016**, *138*, 4657.

[92] N. Liang, D. Meng, Z. Ma, B. Kan, X. Meng, Z. Zheng, W. Jiang, Y. Li, X. Wan, J. Hou, W. Ma, Y. Chen, Z. Wang, *Adv. Energy Mater*. **2017**, *7*, 1601664.

[93] Y. Li, X. Liu, F.-P. Wu, Y. Zhou, Z.-Q. Jiang, B. Song, Y. Xia, Z.-G. Zhang, F. Gao, O. Inganäs, Y. Li, L.-S. Liao, *J. Mater. Chem. A* **2016**, *4*, 5890.

[94] P. Cheng, M. Zhang, T. K. Lau, Y. Wu, B. Jia, J. Wang, C. Yan, M. Qin, X. Lu, X. Zhan, *Adv. Mater.* **2017**, *29*, 1605216.

[95] Y. Cui, H. Yao, C. Yang, S. Zhang, J. Hou, *Acta Polym. Sin.* **2018**, *2*, 1.

Different optical gap definitions and how these different definitions affect the quantification of voltage losses are discussed. By combining the voltage losses summarized from the different optical gap definitions and the efficiency potential simulation, it is predicted that an efficiency of ~18% is expectable for organic solar cells in the future.

Key words: Solar cells, optical gap, voltage losses, Shockley-Queisser limit, Efficiency prediction

Yuming Wang, Deping Qian, Yong Cui, Huotian Zhang, Jianhui Hou, Koen Vandewal, Thomas Kirchartz*, Feng Gao*

Optical Gaps of Organic Solar Cells as a Reference for Comparing Voltage Losses